

Are Zr<sub>6</sub>-based MOFs water stable? Linker hydrolysis vs. capillary-force-driven channel collapse†Cite this: *Chem. Commun.*, 2014, 50, 8944Received 1st April 2014,  
Accepted 20th June 2014

DOI: 10.1039/c4cc02401j

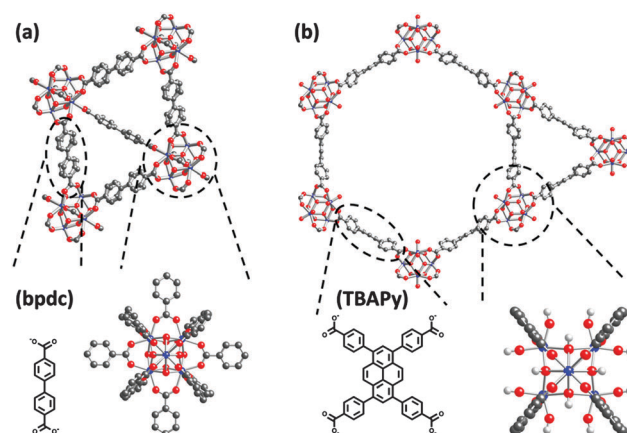
www.rsc.org/chemcomm

Joseph E. Mondloch,<sup>a</sup> Michael J. Katz,<sup>a</sup> Nora Planas,<sup>b</sup> David Semrouni,<sup>b</sup> Laura Gagliardi,<sup>b</sup> Joseph T. Hupp<sup>\*a</sup> and Omar K. Farha<sup>\*ac</sup>

Metal–organic frameworks (MOFs) built up from Zr<sub>6</sub>-based nodes and multi-topic carboxylate linkers have attracted attention due to their favourable thermal and chemical stability. However, the hydrolytic stability of some of these Zr<sub>6</sub>-based MOFs has recently been questioned. Herein we demonstrate that two Zr<sub>6</sub>-based frameworks, namely UiO-67 and NU-1000, are stable towards linker hydrolysis in H<sub>2</sub>O, but collapse during activation from H<sub>2</sub>O. Importantly, this framework collapse can be overcome by utilizing solvent-exchange to solvents exhibiting lower capillary forces such as acetone.

Metal–organic frameworks (MOFs) are a rapidly growing class of porous solid-state materials built up from inorganic nodes and organic linkers.<sup>1</sup> An important and emerging area of interest has been assessing the stability of MOFs. Surprisingly, of the approximately 20 000 known MOFs,<sup>2</sup> only a few dozen exhibit both the thermal and chemical stability desired for certain applications (such as catalysis in harsh environments).<sup>3</sup> Examples of unusually stable MOFs include various zeolitic imidazolate frameworks (ZIFs),<sup>4</sup> MILs,<sup>5</sup> pyrazolate containing frameworks,<sup>6</sup> and MOFs constructed from Zr<sub>6</sub>-based nodes and carboxylate-terminated linkers.<sup>3</sup> The prototypical example is UiO-66, a MOF built up from Zr<sub>6</sub>(O)<sub>4</sub>(OH)<sub>4</sub> nodes and benzene dicarboxylate linkers; UiO-66 is thermally (up to 500 °C),<sup>3</sup> mechanically,<sup>7</sup> hydrolytically, and chemically stable in a variety of organic solvents as well as acidic and basic aqueous media.<sup>3,8</sup> The stability of Zr<sub>6</sub>-based MOFs is attributed to the highly oxophilic nature of the Zr<sup>IV</sup> sites and their Coulombic interaction with negatively charged termini of linkers.

Despite this, the hydrolytic stability of some Zr<sub>6</sub>-based MOFs has recently come in to question. For example, it was reported



Scheme 1 Idealized molecular representations of (a) UiO-67 and (b) NU-1000.

that UiO-67 (Scheme 1)—a MOF isorecticular with UiO-66, but containing extended biphenyl dicarboxylate (bpdc) linkers—is not stable to H<sub>2</sub>O exposure.<sup>8,9</sup> This lack of stability was attributed to linker hydrolysis engendered by clustering of H<sub>2</sub>O molecules near the Zr<sub>6</sub>-based node (a phenomenon observed for other carboxylate containing MOFs<sup>10</sup>) and rotational effects of the extended linker.<sup>8</sup> In contrast to these observations, others have found excellent hydrolytic stability in Zr<sub>6</sub>-based MOFs with linkers of similar length to bpdc and even in MOFs with larger linkers and hence pores.<sup>11</sup>

In the context of our labs' recent efforts utilizing Zr<sub>6</sub>-based MOFs,<sup>12</sup> as well as our continuing efforts to elucidate the effects of activation on the stability and porosity of MOFs,<sup>13</sup> we hypothesized that failures at the activation stage, as opposed to inherent hydrolytic Zr–carboxylate bond stability, could be the cause of the reported degradation of various Zr<sub>6</sub>-based MOFs. Recall that activation entails removing guest molecules, such as solvent or other chemicals utilized during synthesis, from the MOF while maintaining its permanent porosity. We find that addressing issues related to activation can often yield permanently porous MOFs. Chief among these issues are destructive

<sup>a</sup> Department of Chemistry, Northwestern University, 2145 Sheridan Road, Evanston, IL 60208, USA. E-mail: j-hupp@northwestern.edu, o-farha@northwestern.edu

<sup>b</sup> Department of Chemistry, Supercomputing Institute & Chemical Theory Center, University of Minnesota, Minneapolis, MN 55455, USA

<sup>c</sup> Department of Chemistry, Faculty of Science, King Abdulaziz University, Jeddah, Saudi Arabia

† Electronic supplementary information (ESI) available. See DOI: 10.1039/c4cc02401j

(i.e., channel-collapsing) capillary forces which are greatest when solvent surface tension is high and when solvent molecules adhere well to MOF cavities or channels (e.g., *via* strong hydrogen bonding). Processes such as solvent-exchange,<sup>14</sup> supercritical CO<sub>2</sub> (scCO<sub>2</sub>) activation,<sup>15</sup> and freeze-drying have all been employed to help avoid channel collapse in MOFs.<sup>16</sup>

Herein we demonstrate that two Zr<sub>6</sub>-based MOFs, UiO-67 and NU-1000, are stable to linker hydrolysis under our experimental conditions. However, both frameworks are susceptible to capillary-force-driven channel collapse when activated directly from H<sub>2</sub>O. Notably this can be overcome by simple solvent-exchange to acetone. Understanding the differences between linker hydrolysis and capillary-force-driven channel collapse will have a profound impact on the practical limitations of these Zr<sub>6</sub>-based MOFs. For example, the former calls into question the viability of these frameworks for applications involving humid atmospheres, chemical catalysis, and electrocatalysis. In contrast, applications like dehumidification based cooling<sup>17</sup> could indeed prove problematic if the H<sub>2</sub>O-condensation limit is reached as capillary forces would then come into play during MOF regeneration.

UiO-67 was synthesized using the procedure recently reported by Katz *et al.*<sup>12b</sup> The resultant powder X-ray diffraction (PXRD) pattern, Fig. 1a black line, nicely matches the simulated pattern of UiO-67 (gray line) confirming the bulk phase purity of the material. Next we placed UiO-67 in H<sub>2</sub>O for 24 h and examined its PXRD pattern. As one might expect given the reported stability of the UiO series,<sup>3</sup> the PXRD pattern is unaltered. However, upon heating the sample to 150 °C under vacuum and removing the H<sub>2</sub>O molecules from the pores of UiO-67 (i.e., activating the sample), a noticeable broadening of the peaks at angles (2θ) of 5.8 and 6.7 degrees was observed along with nearly complete disappearance of the peaks at higher 2θ (Fig. 1a, red trace). We suspected this loss of crystallinity was due to capillary forces that in turn cause partial or complete framework collapse during activation. To circumvent this problem we exchanged the H<sub>2</sub>O molecules to acetone and subsequently activated the sample thermally (Fig. 1a, blue line).

Pleasingly the crystallinity of UiO-67 was maintained after solvent-exchange to acetone. We also rigorously quantified the relative crystallinity for these UiO-67 samples (and NU-1000, *vide infra*) in the ESI.†

To further elucidate the effects of activating UiO-67 from both H<sub>2</sub>O and acetone, N<sub>2</sub> adsorption isotherms of thermally activated UiO-67 (i.e., DMF synthesis solvent evacuated), a sample activated directly from H<sub>2</sub>O, and a sample activated *via* solvent-exchange to acetone (Fig. 1c) were measured. Activation directly from H<sub>2</sub>O (red triangles) leads to a complete loss of porosity. However, when solvent-exchange to acetone is utilized the porosity of UiO-67 is retained, Fig. 1c (comparison of black circles and blue squares).

Next we turned our attention to the MOF NU-1000 ([Zr<sub>6</sub>(OH)<sub>16</sub>(TBAPy)<sub>2</sub>]) which is built up from Zr<sub>6</sub>(OH)<sub>16</sub> containing nodes and 1,3,6,8-tetrakis(benzoate)pyrene (TBAPy) linkers (Scheme 1).<sup>12a</sup> NU-1000 has triangular micropores as well as exceptionally large mesopores (*ca.* 30 Å diameter). In this regard, NU-1000 should facilitate the permeation of H<sub>2</sub>O throughout its structure and ensure H<sub>2</sub>O molecules can readily access its node. Using the procedure detailed by Mondloch *et al.*,<sup>12a</sup> NU-1000 was synthesized as a microcrystalline powder. The PXRD pattern and N<sub>2</sub> adsorption isotherms are shown in Fig. 1b and d (black line and black circles). Examination of the PXRD patterns of NU-1000 soaked in H<sub>2</sub>O for 24 h but not activated (Fig. 1b, green a line), activated directly from H<sub>2</sub>O (Fig. 1b, red line), and solvent-exchanged to acetone followed by thermal activation (Fig. 1b, blue line) reveal that the crystallinity is maintained except when NU-1000 is activated directly from H<sub>2</sub>O. In particular the reflections centered at 5 and 7.5 degrees have broadened, while the peaks at higher angles have decreased in intensity. Consistent with the UiO-67 sample, N<sub>2</sub> adsorption isotherms (Fig. 1d) demonstrate that the sample activated directly from H<sub>2</sub>O (Fig. 1d, red triangles) exhibits significantly less porosity than either the pristine NU-1000 sample or the one activated *via* solvent-exchange (Fig. 1d, black circles and blue squares). For example, the BET surface area of the sample activated from H<sub>2</sub>O is 480 m<sup>2</sup> g<sup>-1</sup>, while pristine NU-1000 has a surface area of 2040 m<sup>2</sup> g<sup>-1</sup>.

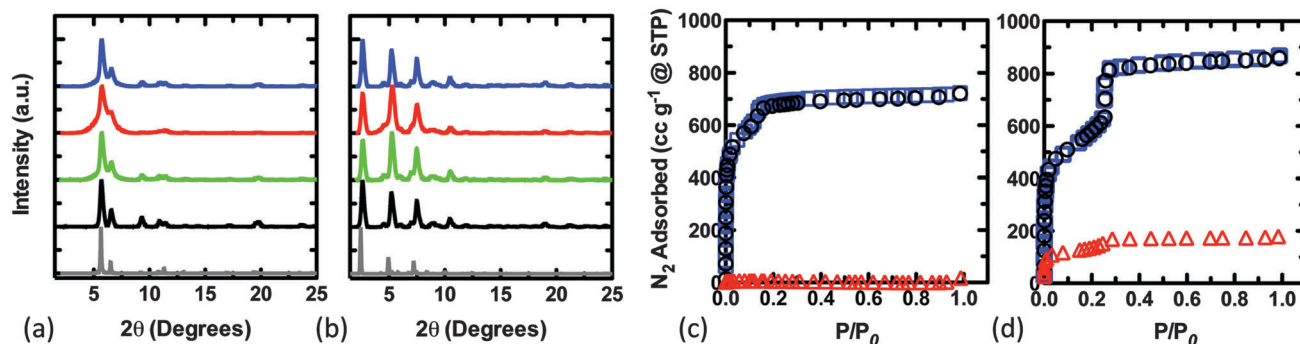


Fig. 1 Normalized PXRD patterns of the simulated structures (gray line), parent MOFs (black line), MOFs in H<sub>2</sub>O (green line), MOFs thermally activated from H<sub>2</sub>O (red line), and MOFs solvent-exchanged to acetone and subsequently activated (blue line) for UiO-67 (a) and NU-1000 (b). For UiO-67 (c) and NU-1000 (d): N<sub>2</sub> adsorption isotherms of samples activated *via* thermal evacuation of the synthesis solvent (DMF or acetone, black circles), thermal evacuation of H<sub>2</sub>O from the pores (red triangles), and exchange of H<sub>2</sub>O for acetone, and then thermal evacuation (blue squares). For clarity only every other data point is displayed in the isotherms.

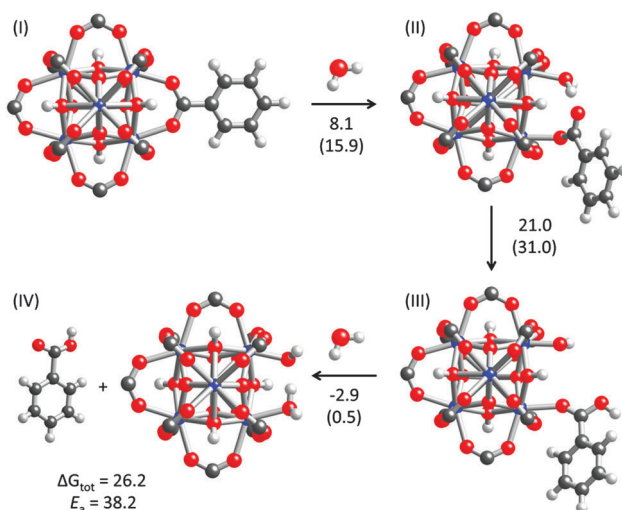


Fig. 2 Molecular representations and DFT free energies (in kcal mol<sup>-1</sup>) associated with the hypothetical hydrolytic degradation of UiO-67. In parenthesis, the corresponding activation free energy.

We further ruled out the hydrolytic pathway in UiO-67 and NU-1000 through a combination of NMR and IR spectroscopies (ESI<sup>†</sup>) as well as quantum chemical characterization. <sup>1</sup>H NMR of the filtrate from the H<sub>2</sub>O soaked samples showed no residual sign of their linkers in solution. Diffuse Reflectance Infrared Fourier Transform Spectroscopy (DRIFTS) demonstrated that both the UiO-67 and NU-1000 frameworks stayed intact after exposure to H<sub>2</sub>O, solvent exchange to acetone, and finally thermally activating the samples. In contrast, DRIFTS of the samples activated directly from H<sub>2</sub>O show broad stretches consistent with the presence of free carboxylates and loss of framework porosity (*i.e.*, node-linker bond breaking occurring during activation). Interestingly we also performed *in situ* DRIFTS experiments (ESI<sup>†</sup>). Exposure of UiO-67 and NU-1000 to H<sub>2</sub>O vapour, followed by removal of excess H<sub>2</sub>O yielded no detectable change in the DRIFTS spectra, a result suggesting that the stability of these frameworks towards H<sub>2</sub>O vapor is different than for condensed phase H<sub>2</sub>O. Finally, cluster model density functional theory, DFT, calculations (at the M06-L level, see ESI<sup>†</sup>) are consistent with the node of UiO-67 being stable towards hydrolytic attack. The computed free energies of the proposed degradation pathway are summarized in Fig. 2; the net free energy is approximately +26 kcal mol<sup>-1</sup> with an overall activation energy of 38 kcal mol<sup>-1</sup>. This is in good agreement with recent calculations from Vermoortele *et al.* demonstrating that removal of CF<sub>3</sub>COO<sup>-</sup> anions from Zr<sub>6</sub> containing nodes is also thermodynamically uphill.<sup>18</sup>

Rather than hydrolytic instability through H<sub>2</sub>O clustering, our data demonstrate instability arises from the presence of capillary forces experienced during activation. Notably, mild activation strategies—such as solvent-exchange (or scCO<sub>2</sub>, no surface tension)—can be utilized to overcome framework collapse. While the surface tension of H<sub>2</sub>O is significantly larger than that of acetone (72 mN m<sup>-1</sup> vs. 26 mN m<sup>-1</sup> at 25 °C),<sup>19</sup> a discussion based on the geometrical properties of the pores of UiO-67 and NU-1000, as well as the literature on confined H<sub>2</sub>O (ESI<sup>†</sup>), brings additional insight into the behaviour of H<sub>2</sub>O molecules and capillary forces in Zr<sub>6</sub>-based MOFs. Although additional data

would be required to quantify these effects, our initial exploration suggests that H<sub>2</sub>O does not behave as a liquid in UiO-67, while it should partially behave as a liquid in the larger pores of NU-1000. This in turn implies that solvent-framework intermolecular forces are significant in driving channel collapse for Zr<sub>6</sub>-based MOFs when activated from H<sub>2</sub>O.

J.T.H., N.P., D.S., and L.G. gratefully acknowledge funding from the U.S. DOE, Office of Basic Energy Sciences, Division of Chemical Sciences, Geosciences and Biosciences (Award DE-FG02-12ER16362). J.E.M., M.J.K., and O.K.F. gratefully acknowledge funding from the Army Research Office (project number W911NF-13-1-0229).

## Notes and references

- (a) O. M. Yaghi, M. O'Keefe, N. W. Ockwig, H. K. Chae, M. Eddaoudi and J. Kim, *Nature*, 2003, **423**, 705; (b) G. Férey, *Chem. Soc. Rev.*, 2008, **37**, 191; (c) S. Horike, S. Shimomura and S. Kitagawa, *Nat. Chem.*, 2009, **1**, 695.
- H. Furukawa, K. E. Cordova, M. O'Keeffe and O. M. Yaghi, *Science*, 2013, **341**, 1230444.
- J. H. Cavka, S. Jakobsen, U. Olsbye, N. Guillou, C. Lamberti, S. Bordiga and K. P. Lillerud, *J. Am. Chem. Soc.*, 2008, **130**, 13850.
- K. S. Park, Z. Ni, A. P. Côté, J. Y. Choi, R. Huang, F. J. Uribe-Romo, H. K. Chae, M. O'Keeffe and O. M. Yaghi, *PNAS*, 2006, **103**, 10186.
- G. Férey, C. Mellot-Draznieks, C. Serre, F. Millange, J. Dutour, S. Surblé and I. Margiolaki, *Science*, 2005, **309**, 2040.
- V. Colombo, S. Galli, H. J. Choi, G. D. Han, A. Maspero, G. Palmisano, N. Masciocchi and J. R. Long, *Chem. Sci.*, 2011, **2**, 1311.
- H. Wu, T. Yildirim and W. Zhou, *J. Phys. Chem. Lett.*, 2013, **4**, 925.
- J. B. Decoste, G. W. Peterson, H. Jasuja, T. G. Glover, Y.-G. Huang and K. S. Walton, *J. Mater. Chem. A*, 2013, **1**, 5642.
- G. C. Shearer, S. Forselv, S. Chavan, S. Bordiga, K. Mathisen, M. Bjørgen, S. Svelle and K. P. Lillerud, *Top. Catal.*, 2013, **56**, 770.
- P. Kùsgens, M. Rose, I. Senkovska, H. Fröde, A. Henschel, S. Siegle and S. Kaskel, *Microporous Mesoporous Mater.*, 2009, **120**, 325.
- (a) W. Morris, B. Voloskiy, S. Demir, F. Gándara, P. L. McGrier, H. Furukawa, D. Cascio, J. F. Stoddart and O. M. Yaghi, *Inorg. Chem.*, 2012, **51**, 6443; (b) H.-L. Jiang, D. Feng, K. Wang, Z.-Y. Gu, Z. Wei, Y.-P. Chen and H.-C. J. Zhou, *J. Am. Chem. Soc.*, 2013, **135**, 13934; (c) D. Feng, W.-C. Chung, Z. Wei, Z.-Y. Gu, H.-L. Jiang, Y.-P. Chen, D. J. Darensbourg and H.-C. Zhou, *J. Am. Chem. Soc.*, 2013, **135**, 17105; (d) D. Feng, Z.-Y. Gu, J.-R. Li, H.-L. Jiang, Z. Wei and H.-C. Zhou, *Angew. Chem., Int. Ed.*, 2012, **51**, 10307; (e) M. Carboni, C. W. Abney, S. Liu and W. Lin, *Chem. Sci.*, 2013, **4**, 2396; (f) Y. Chen, T. Hoang and S. Ma, *Inorg. Chem.*, 2012, **51**, 12600.
- (a) J. E. Mondloch, W. Bury, D. Fairen-Jimenez, S. Kwon, E. J. DeMarco, M. H. Weston, A. A. Sarjeant, S. T. Nguyen, P. C. Stair, R. Q. Snurr, O. K. Farha and J. T. Hupp, *J. Am. Chem. Soc.*, 2013, **135**, 10294; (b) M. J. Katz, Z. J. Brown, Y. J. Colón, P. W. Siu, K. A. Scheidt, R. Q. Snurr, J. T. Hupp and O. K. Farha, *Chem. Commun.*, 2013, **49**, 9449; (c) M. J. Katz, J. E. Mondloch, R. K. Totten, J. K. Park, S. T. Nguyen, O. K. Farha and J. T. Hupp, *Angew. Chem., Int. Ed.*, 2013, **53**, 497.
- (a) O. K. Farha and J. T. Hupp, *Acc. Chem. Res.*, 2010, **43**, 1166; (b) J. E. Mondloch, O. Karagiari, O. K. Farha and J. T. Hupp, *CrystEngComm*, 2013, **15**, 9258; (c) O. K. Farha, A. Ö. Yazaydin, I. Eryazici, C. D. Malliakas, B. G. Hauser, M. G. Kanatzidis, S. T. Nguyen, R. Q. Snurr and J. T. Hupp, *Nat. Chem.*, 2010, **2**, 944; (d) O. K. Farha, I. Eryazici, N. C. Jeong, B. G. Hauser, C. E. Wilmer, A. A. Sarjeant, R. Q. Snurr, S. T. Nguyen, A. Ö. Yazaydin and J. T. Hupp, *J. Am. Chem. Soc.*, 2012, **134**, 15016.
- H. Li, M. Eddaoudi, M. O'Keeffe and O. M. Yaghi, *Nature*, 1999, **402**, 276.
- A. P. Nelson, O. K. Farha, K. L. Mulfort and J. T. Hupp, *J. Am. Chem. Soc.*, 2009, **131**, 458.
- L. Ma, A. Jin, Z. Xie and W. Lin, *Angew. Chem., Int. Ed.*, 2009, **48**, 8905.
- H. Furukawa, F. Gándara, Y.-B. Zhang, J. Jiang, W. L. Queen, M. R. Hudson and O. M. Yaghi, *J. Am. Chem. Soc.*, 2014, **136**, 4369.
- F. Vermoortele, B. Bueken, G. Le Bars, B. Van de Voorde, M. Vandichel, K. Houthoofd, A. Vimont, M. Daturi, M. Waroquier, V. Van Speybroeck, C. Kirschhock and D. E. De Vos, *J. Am. Chem. Soc.*, 2013, **135**, 11465.
- Handbook of Chemistry and Physics*, Chemical Rubber Publishing Company, Boca Taton, FL, 2003.